

Isochronal chaos synchronization of delay-coupled optoelectronic oscillatorsLucas Illing,^{*} Cristian D. Panda, and Lauren Shareshian*Department of Physics, Reed College, Portland, Oregon 97008, USA*

(Received 5 March 2011; revised manuscript received 15 June 2011; published 19 July 2011)

We study experimentally chaos synchronization of nonlinear optoelectronic oscillators with time-delayed mutual coupling and self-feedback. Coupling three oscillators in a chain, we find that the outer two oscillators always synchronize. In contrast, isochronal synchronization of the mediating middle oscillator is found only when self-feedback is added to the middle oscillator. We show how the stability of the isochronal solution of any network, including the case of three coupled oscillators, can be determined by measuring the synchronization threshold of two unidirectionally coupled systems. In addition, we provide a sufficient condition that guarantees global asymptotic stability of the synchronized solution.

DOI: [10.1103/PhysRevE.84.016213](https://doi.org/10.1103/PhysRevE.84.016213)

PACS number(s): 05.45.Xt, 42.65.Sf, 89.75.-k

I. INTRODUCTION

When systems are coupled, their interaction often leads to correlations in their dynamics. This is true even for coupled chaotic oscillators, where an exchange of signals that are a function of the oscillator's internal states can lead to identical chaotic trajectories [1–3].

Typically, coupling oscillators together introduces time delays because of the finite propagation speed of the exchanged signals. This is particularly true for optical and optoelectronic devices that operate at technologically relevant radio frequencies of several GHz.

For unidirectionally coupled systems, coupling delays impose no additional obstacles to chaos synchronization and a large body of experimental research exists that demonstrates identical chaotic dynamics of two coupled photonic systems [4,5]. In contrast, for mutually coupled systems or networks with feedback loops, the presence of such propagation delays can pose fundamental challenges to synchronization. Nevertheless, experimental investigations using laser systems have shown that, in addition to lag and anticipatory synchronization [6–9], isochronal (or zero-lag) synchronization is possible [10–13]. In this case, somewhat counterintuitively, chaotic units synchronize without any relative time delay, although the transmitted signal is received with a large time lag. It is not immediately obvious what conditions lead to isochronal synchronization, either of parts of a network or the entire network. This is the question we address in this paper.

Detailed investigations of chaos synchronization of two nominally identical mutually delay-coupled semiconductor lasers showed that, in such a system, the isochronal solution exists but is unstable and therefore not observable [6–8,14]. Instead “achronal” synchronized behavior is found, where the two lasers show similar but nonidentical behavior and where they are delayed with respect to each other by the coupling time. Under detuned operation, the laser with higher optical frequency leads the dynamics, while for zero detuning the two lasers spontaneously switch leader and laggard roles [6,7,15]. Achronal synchronization and leader-laggard switching has also been demonstrated using mutually coupled fiber ring lasers [16,17].

It has been found that stable isochronal synchronization can be achieved through the introduction of several incommensurate time delays [18], delayed shared feedback coupling [19], the inclusion of a mediating, yet unsynchronized, center laser [13], and through the addition of self-feedback [10–12]. Experimentally, the stabilizing effect of self-feedback has been demonstrated for the case of two incoherently [12] as well as two coherently [11] coupled semiconductor lasers. In addition, numeric calculations demonstrated the stabilizing effect of self-feedback for three coupled fiber ring lasers and it has been suggested to be a general phenomenon [10].

In this paper, we go beyond the case of two coupled chaotic units and investigate the synchronization properties of three mutually coupled optoelectronic oscillators, devices that are known to generate fast high-dimensional chaos [20,21]. We show that when a center unit with self-feedback is introduced, thereby forming a chain of three coupled oscillators, as described in Sec. II, not only are the outer two oscillators always in isochronal synchrony (Sec. III), but the entire chain can be synchronized for sufficient self-feedback strength (Sec. IV). Since the chaotic dynamics and theoretical description of our optoelectronic oscillators is different from those of the semiconductor lasers used in most of the previous research, our findings support theoretical arguments suggesting that the stabilizing effect of self-feedback [10] and the synchronization via a mediating center oscillator [22,23] are general phenomena that are mainly a result of the network structure and largely independent of the node dynamics. In addition, we provide a sufficient condition that guarantees isochronal synchrony. More importantly, we show in Sec. V that the stability of the fully synchronized state of any network, including the case of three mutually coupled oscillators, is predicted by the dynamics of two unidirectionally coupled systems.

II. EXPERIMENTAL SETUP AND MODEL

The experimental setup, shown in Fig. 1, involves three mutually coupled optoelectronic oscillators in a chain configuration. Each node in the chain consists of a nonlinear device that maps an electronic input to an optical output. The three-node delay-coupled network is formed by converting the optical outputs to amplified, linearly filtered, and time-delayed electrical signals that serve as inputs to the nonlinearities.

^{*}illing@reed.edu

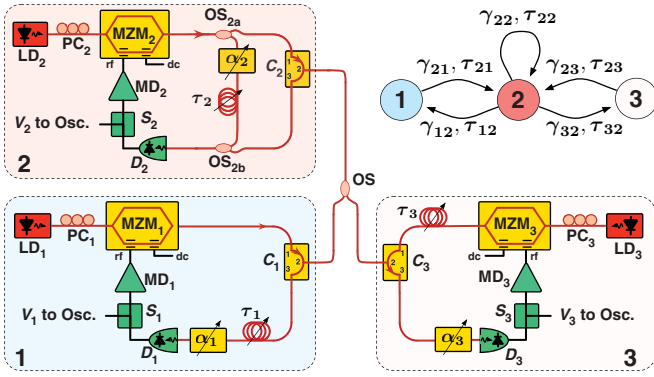


FIG. 1. (Color online) Schematic of the experiment consisting of three coupled optoelectronic oscillators: LD, laser diodes; PC, polarization controllers; MZM, Mach Zehnder modulators; C, optic circulators; OS, optical splitters; α , adjustable optic attenuators; τ , adjustable optical fiber delay lines; D, photodetectors; S, electronic splitters; MD, modulator drivers. (Inset) Coupling architecture.

Oscillations arise due to the interplay of the nonlinear mapping, filtering, and time delay.

In more detail, in each oscillator constant optical power is provided by a continuous-wave 1.55 μm fiber-coupled semiconductor laser. The crucial nonlinear transformation is performed by a LiNbO₃ Mach-Zehnder modulator (MZM) that maps a radio-frequency voltage applied to its ac-coupled input port ($V_{\pi,\text{rf}} = 4.5 \text{ V}$) to a time varying optical output. Taking into account the amplification and saturation ($V_{\text{sat}} = 4.9 \text{ V}$) of the inverting modulator driver (MD) (gain $g_{\text{MD}} = -23$) attached to the MZM rf-input port, the nonlinear transformation can be described by the normalized output function [21]

$$h[x] = \frac{\cos(m + d \tanh[x])^2 - \cos(m)^2}{d |\sin(2m)|}, \quad (1)$$

where $d = \pi V_{\text{sat}}/2V_{\pi,\text{rf}}$ is a constant and $x_i = g_{\text{MD}} V_i/V_{\text{sat}}$ denotes the dimensionless and scaled variable corresponding to the measured output voltage. The bias m is set by applying a dc voltage to a second port on the MZM. For all experiments discussed in this paper, we bias to the half-transmission point with positive slope, $m = -\pi/4$. For this bias, function (1) simplifies to

$$h[x] = \frac{\sin(2d \tanh[x])}{2d}. \quad (2)$$

The optical output of each MZM is routed via circulators (C) and an optical splitter (OS) toward the other MZMs. For example, light exiting MZM₁ enters port one of circulator C₁ and is routed to port three of circulator C₂. The optical power in the fibers is then converted to a voltage by broadband amplified photodetectors (bandwidth 30 kHz–13 GHz). Half of the resulting signals, denoted by V_i ($i = 1, 2, 3$), is measured by a 12-GHz real-time digital oscilloscope. The other half serves as input to the modulator drivers, thereby closing the system.

The photodetectors are the main bandwidth limiting components. Due to their ac coupling, they act as bandpass filters, a fact that has to be taken into account when modeling the optoelectronic oscillators [24,25]. Good agreement between experiment and theory has been found when a simple two-pole bandpass filter description of the linear frequency response is

used, resulting in a second-order delay-differential equation (DDE) model for the feedback system [20,21]. Adapting such a model, with a high-(low-)frequency cutoff $\omega_+ \approx 7 \times 10^{10} \text{ s}^{-1}$ ($\omega_- \approx 2 \times 10^5 \text{ s}^{-1}$), center frequency $\omega_0 = \sqrt{\omega_+\omega_-} = 1.2 \times 10^8 \text{ s}^{-1}$, and bandwidth $\delta \approx \omega_+$, one obtains the following dimensionless set of coupled DDEs describing the dynamics of a network of three oscillators:

$$\dot{\mathbf{z}}_i(t) = \mathbf{A} \cdot \mathbf{z}_i(t) + \mathbf{b}g_0 \sum_{j=1}^3 \gamma_{ij} h[x_j(t - \tau_{ij})]. \quad (3)$$

Here, $i \in \{1, 2, 3\}$ labels the oscillators and the second-order DDE for each is written in terms of two variables, $\mathbf{z}_i = (x_i, y_i) \in \mathbb{R}^2$, where $y_i = \omega_0^2/\delta \int_{t_0}^t x_i(\ell) d\ell$ [20,21]. In Eq. (3), time is measured in units of the fast time constant associated with the device component's high frequency cutoff and is defined as $t = \text{time} \times \delta$. The overdot in Eq. (3) denotes the derivative with respect to this dimensionless time and $\tau_{ij} = T_{ij}\delta$ is the dimensionless propagation time of a signal traveling from oscillator j to oscillator i . In the experiment, the propagation times T_{ij} are adjusted using optical fiber delay lines to an absolute precision given by our measurement uncertainty of 0.1 ns. Relative to one another, the delays can be matched to about 10 ps. The constant matrix \mathbf{A} ,

$$\mathbf{A} = \begin{bmatrix} -1 & -1 \\ \epsilon & 0 \end{bmatrix},$$

with small parameter $\epsilon = \omega_0^2/\delta^2$ characterizes the bandpass filter. The constant coupling vector \mathbf{b} is $\mathbf{b} = (1, 0)^T$, and the scalar output function h is given by Eq. (2). Note that h is defined such that $h[0] = 0$ and $\partial h/\partial x[0] = 1$, which implies that $x = y = 0$ is a steady state solution of Eq. (3) and that $g_0\gamma_{ij}$ is the gain a small signal of frequency ω_0 experiences when injected into system j and measured at the output of system i . Tuning either the adjustable attenuators or the laser powers, the magnitude of the coupling coefficients can be varied between zero and one ($0 \leq \gamma_{ij} \leq 1$). For all data shown in this paper, the maximum small signal gain was kept constant for all links at a value of $g_0 = 6.1$. For this gain and a delay time of $T = 81.3 \text{ ns}$ ($\tau = 5622$), a single oscillator with self-feedback exhibits high-dimensional chaos [20,21,26].

The symmetry of the experimental setup implies that the relevant synchronized solutions are the partially synchronized solution, where the two outer oscillators exhibit identical dynamics and the fully synchronized solution, where all three oscillators behave identically.

III. CLUSTER SYNCHRONIZATION

The case where isochronal synchronization between the two outer delay-coupled oscillators is achieved through relaying their dynamics via a third mediating but unsynchronized element was first discovered in a system of three semiconductor lasers coupled via mutual optical injection by Fischer *et al.* [13]. In the context of general networks of coupled oscillators, this type of synchronization can be seen as the simplest possible example of cluster synchronization [27].

In our experimental system of coupled optoelectronic oscillators, we also observe cluster synchronization, in spite of the fact that our setup exhibits dynamics that are quite

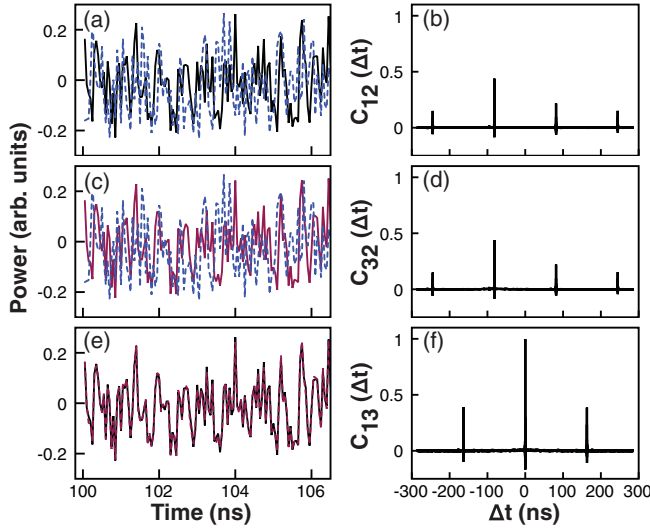


FIG. 2. (Color online) Experimental time series (a),(c),(e) and cross-correlation plots (b),(d),(f) for three oscillators in a chain without self-feedback. (a),(b) Oscillator 1 (black solid line) and 2 (blue dashed line), (c),(d) oscillator 3 (magenta solid line) and 2 (blue dashed line), and (e),(f) oscillator 1 (black solid line) and 3 (magenta dashed line) with a cross-correlation that has a maximum of 0.99 at $\Delta t = 0$.

distinct from those of the semiconductor lasers used by Fischer *et al.* [13]. An example of cluster synchronization arising in our experiments is shown in Fig. 2 for a setup where there is no self-feedback ($\gamma_{ii} = 0$), all delays are equal with $T_{ij} = T = 81.3$ ns ($\tau_{ij} = 5622$), and the cross-coupling strengths are balanced ($\gamma_{12} = \gamma_{32} = 1$ and $\gamma_{21} = \gamma_{23} = 1/2$). As seen in Figs. 2(e) and 2(f), the outer two oscillators are synchronized perfectly without any time shift. In contrast, no (identical) synchronization occurs between either of the outer two oscillators and the mediating middle one [see Figs. 2(a)–2(d)]. In this case, signals are most similar when shifted by the coupling delay, as seen by the correlation peaks at time shifts of $\pm T$.

To analytically investigate synchrony between the outer two oscillators, consider the difference

$$\eta(t) = \mathbf{z}_1(t - \tau_{32} + \tau_{12}) - \frac{\gamma_{12}}{\gamma_{32}} \mathbf{z}_3(t), \quad (4)$$

where the delay $\tau_{32} - \tau_{12}$ is the trivial time shift that arises if the propagation times from the middle oscillator to the outer oscillators are not perfectly matched and the factor γ_{12}/γ_{32} is the trivial amplitude scaling that arises if the coupling strengths of the links from the middle oscillator to the outer oscillators differ. We consider the outer two oscillators to be isochronally synchronized if $\eta = 0$, even for cases where the trivial time shift is nonzero or the scaling factor is unequal to one. The evolution of η is described by

$$\dot{\eta}(t) = \mathbf{A}\eta(t). \quad (5)$$

Not only is $\eta(t) = 0$ always a solution, but it is unconditionally globally stable, because the matrix \mathbf{A} , representing the filter, has eigenvalues with strictly negative real parts. Thus the outer two oscillators always synchronize. Neither the coupling delays nor the coupling strengths need to be matched, despite

the mutual coupling between the outer and the middle oscillator. The only requirement is that the outer two systems are identical.

For nondissipative coupling, as in our experiment, a necessary condition for identical synchronization of the outer oscillators is that each system without input is dissipative, i.e., its dynamics decays to $\mathbf{z} = 0$ for $\gamma_{ij} = 0$. This property is necessary in order to allow systems that start with different initial conditions to approach one and the same trajectory as a function of time. For our optoelectronic oscillators, the internal dynamics is not only dissipative but is that of a linear filter, resulting in unconditional stability. Therefore, optoelectronic oscillators are an especially simple case. For other systems, such as optically coupled semiconductor lasers [13], where the internal dynamics is described by a nonlinear dissipative equation, the isochronal partial synchronized solution is not unconditionally stable. Nevertheless, isochronal chaos synchronization of the outer two systems is thought to be a general phenomenon if the delays are sufficiently large [22,23]. The main idea is that synchronization can be expected if all nodes of a network subgroup receive the same input signals and if the nodes are known to exhibit generalized synchronization [28,29] when driven by their own dynamics. This argument for isochronal synchronization of a node subgroup assumes that no essential change of the dynamic behavior arises due to mutual coupling, which, unlike the driven case, allows an oscillator on a particular network node to act back on itself after a time of twice the coupling delay. The argument therefore relies on short autocorrelation times of chaotic systems in combination with long coupling delays and is not expected to apply directly to periodic oscillations, where resonant effects have to be taken into account [22]. In contrast, the unconditionally stable optoelectronic oscillators synchronize not only for chaotic but for any form of node dynamics.

IV. ISOCHRONAL SYNCHRONIZATION

Without any self-feedback, isochronal synchronization of all three optoelectronic oscillators is never observed in our experiments. However, if sufficient self-feedback is added to the middle oscillator, we find stable isochronal synchronization of the entire three-node network. This is shown in Fig. 3(a), where for strong self-feedback ($\gamma_{22} = 0.9$) the measured output of the left outer oscillator is plotted versus the output of the middle oscillator, resulting in a diagonal line, which indicates nearly identical (chaotic) dynamics. The corresponding correlation coefficient is $C_{12} = 0.985$.

In terms of the model, complete isochronal synchronization occurs when $\mathbf{s}(t) := \mathbf{z}_1(t) = \mathbf{z}_2(t) = \mathbf{z}_3(t)$. This solution to Eq. (3) exists if all time delays are identical and if the sum of the input coupling strengths is identical for each oscillator, i.e., if the coupling matrix with matrix elements γ_{ij} has unity row sum for all rows.

Based on this row-sum condition, one would expect to observe maximum correlation between the outer and the middle oscillators for coupling strengths satisfying $1 = \gamma_{21} + \gamma_{22} + \gamma_{23}$. This is exactly what we find experimentally, as is shown in Fig. 3(b), where the maximum of the correlation curve coincides with the dashed line indicating the value of $\gamma_{21} + \gamma_{23}$ required by the row-sum condition.

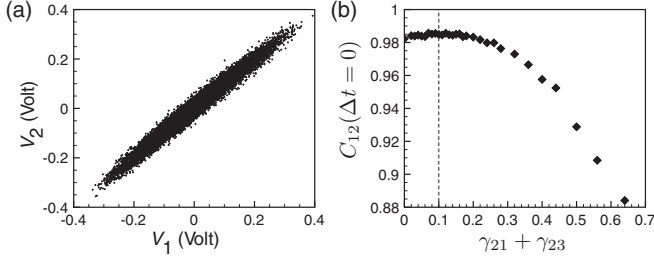


FIG. 3. Experiment with self-feedback, $\gamma_{22} = 0.9$: (a) Output voltage $V_1(t)$ vs $V_2(t)$ for matched delays and coupling coefficients $\gamma_{12} = \gamma_{32} = 1$ and $\gamma_{21} = \gamma_{23} = 0.05$. (b) Correlation coefficient as a function of the strength of the coupling to the middle oscillator from the outer oscillators, $\gamma_{21} + \gamma_{23}$.

Yet, even if the conditions for existence are met, the synchronized solution is clearly not always stable. Thus we address next the crucial question of stability of the isochronal solution. To simplify the discussion we consider, without loss of generality, the symmetric setup where $\gamma_{12} = \gamma_{32} = 1$, the self-feedback strength of the middle oscillators is $\gamma_{22} = \kappa$, and $\gamma_{21} = \gamma_{23} = (1 - \kappa)/2$.

The experimental results for this setup are shown in Fig. 4(a) as circles, where we plot the correlation coefficient of the measured output of the left outer and the middle oscillator for different self-feedback strengths κ . It is seen that high quality isochronal synchronization is found for self-feedback strengths as low as $\kappa \approx 0.7$. For smaller self-feedback, the correlation rapidly drops. The range of κ over which the systems synchronize depends on the gain g_0 . Generally, we find narrower synchronization regimes for higher values of g_0 , where larger g_0 also correspond to higher Lyapunov dimensions of the chaotic attractor of a single system with self-feedback.

Numerical simulations of the three oscillator network as described by Eq. (3) yield qualitatively identical results to the experiments, as seen in Fig. 4(b). Starting from random initial conditions, all three oscillators synchronize for sufficiently large κ . The somewhat larger synchronization region, with a lower bound of $\kappa \approx 0.5$ for the required self-feedback strength, is expected because the simulations are free of noise and parameter mismatches. Based on these results, we believe that Eq. (3) provides a reasonably accurate model of our experiment.

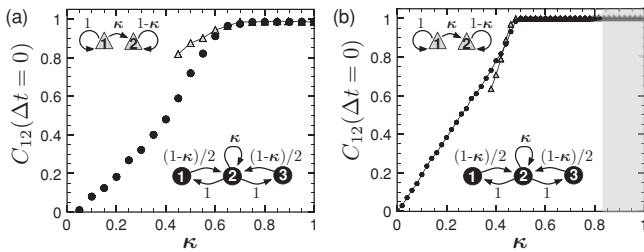


FIG. 4. Correlation coefficient as a function of self-feedback strength κ for the mutually coupled three-oscillator network (black circles) and unidirectionally coupled two-oscillator network (gray triangles). (a) Experimental results; (b) numerics. In the shaded region, the synchronized solution is globally asymptotically stable.

In the following, we use Eq. (3) to derive a global stability bound and to show how to determine the critical self-coupling strength.

When investigating isochronal synchronization of the three-oscillator network analytically, it suffices to consider the evolution of the difference between one of the outer oscillators and the middle oscillator, e.g., $\Delta = \mathbf{z}_1 - \mathbf{z}_2$, because the outer two oscillators will always synchronize, as shown in Sec. III. This difference evolves according to

$$\dot{\Delta} = \mathbf{A} \cdot \Delta - \mathbf{b}g_0(1 - \kappa)f[x_2(t - \tau), \Delta_x(t - \tau)], \quad (6)$$

where $\Delta = (\Delta_x, \Delta_y)$ and the nonlinear function f is defined as

$$f[x_2, \Delta_x] = h[x_2 + \Delta_x] - h[x_2], \quad (7)$$

with h given by Eq. (2). Utilizing the fact that $f[x_2, 0] = 0$ and $|f[x_2, \Delta_x]| \leq |\Delta_x|$, one can apply a variation on the method of Lyapunov-Krasovskii functionals (see the Appendix) to show that the synchronized solution ($\Delta = 0$) is globally asymptotically stable if

$$1 - \frac{1}{g_0} \leq \kappa. \quad (8)$$

Here, $g_0 > 1$ is assumed, since for smaller values of g_0 no oscillations exist that could be synchronized because the steady-state solution for a single oscillator with self-feedback is globally asymptotically stable [24,30]. For the value of g_0 corresponding to the experiments, Eq. (8) implies $\kappa > 0.83$.

It is seen in Fig. 4 that isochronal synchronization occurs over the predicted range, yet the experimental and numerical data also show that Eq. (8) is a conservative bound. As is often the case, the global result does not provide a good estimate of the synchronization threshold. Nevertheless, global stability results are useful because they guarantee synchronization.

To obtain a tight bound on the required self-feedback strength κ , we consider the local stability of the synchronization manifold, taking the usual stability criterion, which requires that the maximum transverse Lyapunov exponent is negative. The transverse Lyapunov exponents are calculated based on solutions of the variational equation corresponding to Eq. (6), which depends on the synchronized trajectory $\mathbf{z}_2(t) = \mathbf{s}(t)$. That is, one determines, for a synchronized pair of outer oscillators, the rates of exponential growth of solutions $\Delta(t)$ of the system of equations

$$\dot{\mathbf{z}}_2 = \mathbf{A} \cdot \mathbf{z}_2 + \mathbf{b}g_0h[x_2(t - \tau)], \quad (9)$$

$$\dot{\Delta} = \mathbf{A} \cdot \Delta + \sigma \mathbf{b}g_0h'[x_2(t - \tau)]\Delta_x(t - \tau), \quad (10)$$

where $\sigma = -(1 - \kappa)$. In this context, it is important to note that although a negative maximum transverse Lyapunov exponent of a typical chaotic trajectory is often found to coincide with the experimentally observed threshold, it is not a sufficient condition for stability of the synchronized solution, as, for example, the basin of attraction might be small or bubbling might occur [31,32]. We numerically calculated the largest transverse Lyapunov exponent using the method first detailed in [33], finding $\lambda_{\perp}^{\max} = -1.3 \times 10^{-4} \text{ ns}^{-1}$ for $\kappa = 0.48$ and $\lambda_{\perp}^{\max} = 0.8 \times 10^{-4} \text{ ns}^{-1}$ for $\kappa = 0.50$. The exponent changes sign for κ slightly less than 0.5 in agreement with the direct

(global) measure of synchronization quality given by the cross-correlation coefficient [see Fig. 4(b)]. This demonstrates that the local stability criterion in terms of the transverse Lyapunov exponent correctly predicts the synchronization threshold.

V. ISOCRONAL SYNCHRONIZATION OF GENERAL NETWORKS

To connect our experiments on three coupled oscillators to the case of general networks, we note that Eqs. (9) and (10) are also obtained when applying to Eq. (3) the master stability function method [34]. In this method, a coordinate transformation to the network eigenmodes is performed that brings the coupling matrix into diagonal form with the result that the stability of each network mode is described by a decoupled equation identical to Eq. (10) with σ replaced by σ_k , the eigenvalue of the k th mode.¹ For any network of identical elements, the master stability function method thereby neatly divides the problem into a part that only depends on the topology of the network, i.e., finding the network eigenvalues σ_k , and a part that only depends on the particular chaotic system at hand, i.e., determining the master stability function, which is nothing but the maximum transverse Lyapunov exponent as a function of the complex parameter σ . The fully synchronized solution is stable if all transversal network eigenvalues fall into regions where the master stability function is negative. Here, transversal eigenvalues are all eigenvalues σ_k , except the one associated with perturbations within the synchronization manifold with corresponding eigenvector $(1, 1, \dots, 1)$.

For the case where the dynamics of a single network element is described by a DDE, the numerical challenge associated with the computation of the master stability function can be drastically reduced for systems with large delay because it was recently shown that, in this case, the master stability function is rotationally symmetric [36]. The maximum transverse Lyapunov exponent only depends on the magnitude of σ . Assuming that the system is stable in the absence of any time-delayed input ($\sigma = 0$), the master stability function is negative in a circular region around the origin with some radius $|\sigma|_c$. This is true not only for chaotic dynamics but also for periodic and steady state behaviors [30,36]. Thus, for DDEs with large delay, it is sufficient to know the largest Lyapunov exponent as a function of positive real-valued σ (or any other convenient radial line in the σ plane).

For the three oscillator network studied in this paper, we find that the spectrum of network eigenvalues contains one unity eigenvalue with associated eigenvector $(1, 1, 1)$, corresponding to perturbations within the synchronization manifold. These perturbations grow exponentially due to the chaotic dynamics, resulting in a positive largest Lyapunov exponent. The remaining eigenvalues are transversal eigenvalues. The second eigenvalue is equal to zero and corresponds to perturbations of the outer two oscillators with respect to one another, resulting in a negative largest (transverse) Lyapunov exponent due to the unconditional global stability, as discussed in Sec. III.

¹For coupling matrices that are not diagonalizable, the master stability function approach can still be applied, as shown, for example, in [35].

The third and final eigenvalue is $\sigma_3 = -(1 - \kappa)$ and this is the relevant network eigenvalue determining the stability of isochronal synchronization, in agreement with Eq. (10).

If the master stability function is rotationally symmetric, the synchronization threshold should be the same if one replaces the negative network eigenvalue $\sigma = \sigma_3 = -(1 - \kappa)$ by a positive one, $\sigma = 1 - \kappa$. We can test this experimentally because such a replacement maps the problem onto that of determining the synchronization region for a setup consisting of two unidirectionally coupled oscillators with self-feedback. In particular, considering Eq. (3) for two oscillators with equal delays and coupling coefficients $\gamma_{11} = 1, \gamma_{12} = 0, \gamma_{21} = \kappa$, and $\gamma_{22} = 1 - \kappa$ yields a system of DDE's for which the solution corresponding to isochronal synchronization of oscillator 1 (master system) and oscillator 2 (driven system) exists and the equations determining the solution's stability are given by Eqs. (9) and (10) with $\sigma = -(1 - \kappa)$ replaced by $\sigma = (1 - \kappa)$.

In Fig. 4(a), we show the results of such a two-oscillator experiment as triangles. It is seen that the region of isochronal synchronization exactly coincides with that of the three-oscillator network. Beyond the synchronization region, equations describing the dynamics of the mutually coupled three-oscillator network and the unidirectionally coupled two-oscillator setup are different and, therefore, one neither expects nor finds a match of the cross correlation coefficients. The experimental results are confirmed by the corresponding numerical simulation shown in Fig. 4(b).

These results show that the theory predicting the rotational symmetry of the master stability function in the limit of infinite delays is applicable, in practice, to systems with finite delay, such as the optoelectronic oscillators in this experiment. What we have demonstrated here is an interesting and useful consequence of the rotational symmetry of the master stability function: one can predict the occurrence of isochronal synchronization in any network of delay-coupled identical oscillators based on the knowledge of synchronization properties of one of the simplest possible setups—that of two unidirectionally coupled oscillators with self-feedback. For the case of the optoelectronic oscillators, our experiments show the synchronization threshold to be $|\sigma|_c \approx 1 - 0.7 = 0.3$, which means that any larger network of such oscillators will exhibit isochronal synchronization only if all transversal network eigenvalues have a magnitude of $|\sigma_k| < 0.3$.

VI. CONCLUSION

In this paper, we have shown through experiments, numerics, and analytic methods that isochronal synchronization of three mutually coupled delay oscillators in a chain configuration can be achieved by adding self-feedback to the center unit, whereas without sufficient self-feedback only the outer two oscillators synchronize. Furthermore, we have demonstrated that isochronal synchronization of any network can be predicted based on measurements of just two unidirectionally coupled oscillators. This amazing simplification is due to the symmetry of the master stability function [36] for delay-coupled networks and relies on the assumptions that identical dynamical systems are used as the network nodes, that

all the delays are equal, and that the only tunable parameters are the external coupling strengths.

ACKNOWLEDGMENTS

This work was supported by the Research Corporation for Science Advancement (Grant No. 7847). L.I. thanks T. Nishikawa for helpful comments.

APPENDIX: GLOBAL STABILITY CONDITION

In this section, we derive the global stability bound given by Eq. (8). The fully synchronized solution is stable if the steady state solution of Eq. (6), i.e., $\mathbf{\Delta}(t) = 0$, is stable. Writing Eq. (6) in terms of its components, $\mathbf{\Delta} = (\Delta_x, \Delta_y)$, yields

$$\begin{aligned}\dot{\Delta}_x &= -\Delta_x - \Delta_y + g_0\sigma f[x_2(t-\tau), \Delta_x(t-\tau)], \\ \dot{\Delta}_y &= \epsilon\Delta_x,\end{aligned}\quad (\text{A1})$$

where $\epsilon \ll 1$, f is defined by Eq. (7), and $\sigma = -(1 - \kappa)$ is the real-valued coupling coefficient.

To prove Eq. (8), we use an extension of the method of Lyapunov-Krasovskii functionals due to Kolmanovskii and Nosov (Theorem 5.7 and 5.8 in [37]). Although in this method two functionals are required to establish asymptotic stability, it has the advantage that it suffices to construct a Lyapunov-Krasovskii functional with a nonpositive derivative.

As the Lyapunov-Krasovskii functional, we use

$$V(t, \mathbf{\Delta}_t) = \Delta_x^2 + \frac{\Delta_y^2}{\epsilon} + \int_{t-\tau}^t f[x_2(s), \Delta_x(s)]^2 ds. \quad (\text{A2})$$

The scalar, continuous, nondecreasing functions $\omega_1(r) = r^2$ and $\omega_2(r) = [(\epsilon)^{-1} + \tau]r^2$, which satisfy $\omega_i(0) = 0$ and $\omega_i(r) > 0$ for $r > 0$, provide bounds for the Lyapunov-Krasovskii functional V ,

$$\omega_1[\|\varphi(0)\|] \leq V(t, \varphi) \leq \omega_2[\|\varphi(\theta)\|], \quad (\text{A3})$$

with $t \geq t_0$, $\varphi(\theta) \in B_H$, and $t_0 \in \mathbb{R}$.

In terms of notation, the argument $\varphi(\theta)$ is understood to denote an element of the Banach space $C = C([- \tau, 0], \mathbb{R}^2)$ of continuous functions mapping the interval $[- \tau, 0]$ ($\tau > 0$) into \mathbb{R}^2 . The norm is defined as $\|\varphi\| = \sup_{-\tau \leq \theta \leq 0} |\varphi(\theta)|$, where $|\cdot|$ is the Euclidean norm in \mathbb{R}^2 . The shorthand $\mathbf{\Delta}_t$ is used to designate for each fixed t the function in C given by $\mathbf{\Delta}_t(\theta) = \mathbf{\Delta}(t + \theta)$, $\theta \in [- \tau, 0]$. Finally, B_H denotes the closed ball of radius H in the Banach space C ,

$$B_H = \{\varphi \in C([- \tau, 0], \mathbb{R}^2), d(0, \varphi) \leq H\},$$

where $d(x, y) = \|x - y\|$ is the distance.

We note that Eq. (A3) holds in any ball B_H and that $\omega_1(r) \rightarrow \infty$ as $r \rightarrow \infty$. This latter property is important because it is used to establish that the asymptotic stability is global.

Next, we make the assumption that

$$1 \geq g_0|\sigma| \quad (\text{assumption}), \quad (\text{A4})$$

where the maximum gain g_0 is positive and real valued. Furthermore, we can take g_0 to be larger than unity, $g_0 > 1$, because otherwise the optoelectronic oscillators will exhibit steady state behavior only [24] and $\mathbf{\Delta}(t) = 0$ is true trivially.

Under assumption (A4), the continuous functional $\bar{\omega}_3(\varphi)$, defined as

$$\bar{\omega}_3(\varphi) = -[1 - g_0|\sigma|][\varphi_x^2(0) + \varphi_x^2(-\tau)], \quad (\text{A5})$$

is nonpositive: $\bar{\omega}_3(\varphi) \leq 0$. Writing x^τ as a shorthand for delayed variables, $x^\tau = x(t - \tau)$, and taking the time derivative of $V(t, \mathbf{\Delta}_t)$ with respect to the trajectories of Eq. (A1), one obtains

$$\begin{aligned}\dot{V}(t, \mathbf{\Delta}_t) &= -(1 - g_0|\sigma|)(\Delta_x^2 + f[x_2^\tau, \Delta_x^\tau]^2) - (\Delta_x^2 - f[x_2, \Delta_x]^2) \\ &\quad - \left(\sqrt{g_0|\sigma|} f[x_2^\tau, \Delta_x^\tau] + \frac{g_0\sigma}{\sqrt{g_0|\sigma|}} \Delta_x \right)^2.\end{aligned}$$

Utilizing the inequality $|f[x_2, \Delta_x]| \leq |\Delta_x|$ yields the estimate

$$\dot{V}(t, \mathbf{\Delta}_t) \leq -(1 - g_0|\sigma|)(\Delta_x^2 + [\Delta_x^\tau]^2) = \bar{\omega}_3(\mathbf{\Delta}_t),$$

demonstrating that the Lyapunov-Krasovskii functional has a nonpositive derivative: $\dot{V}(t, \mathbf{\Delta}_t) \leq \bar{\omega}_3(\mathbf{\Delta}_t) \leq 0$.

The above inequalities guarantee that system trajectories hit the neighborhood of the zero set

$$Q(\bar{\omega}_3 = 0) = \{\varphi \in B_H, \bar{\omega}_3(\varphi) = 0\}, \quad (\text{A6})$$

where the neighborhood $E(\mu, \rho) \subseteq C([- \tau, 0], \mathbb{R}^2)$ is defined by

$$E(\mu, \rho) = \{\varphi \in B_H, d(\varphi, Q) \leq \rho, \mu \leq \|\varphi\| \leq H\}.$$

For the case at hand, the set Q consists of elements $\mathbf{\Delta}_t = [\Delta_x(t + \theta), \Delta_y(t + \theta)]^T \in C([- \tau, 0], \mathbb{R}^2)$ with

$$\Delta_x(t - \tau) = \Delta_x(t) = 0 \quad (\text{A7})$$

and the definition of the neighborhood $E(\mu, \rho)$ implies the inequalities $|\Delta_x(t)| \leq \rho$, $|\Delta_x(t - \tau)| \leq \rho$, and $\mu^2 \leq \Delta_y(t)^2 \leq H^2$. Although the set Q contains the origin, it does not coincide with the origin. One therefore utilizes a second functional to show asymptotic stability. Consider as the second functional

$$W(\mathbf{\Delta}_t) = \Delta_x(t)\Delta_y(t), \quad (\text{A8})$$

which is seen to be bounded in any ball B_H . An upper bound for the time derivative of W in $E(\mu, \rho)$ is obtained by using assumption (A4) and the inequality $|f[x_2, \Delta_x]| \leq |\Delta_x|$,

$$\begin{aligned}\dot{W} &= -\Delta_x\Delta_y - \Delta_y^2 + \sigma g_0 f[x_2^\tau, \Delta_x^\tau]\Delta_y + \epsilon\Delta_x^2 \\ &\leq |\Delta_x||\Delta_y| - \Delta_y^2 + |\Delta_x^\tau||\Delta_y| + \epsilon\Delta_x^2 \\ &\leq \rho H - \mu^2 + \rho H + \epsilon\rho^2.\end{aligned}\quad (\text{A9})$$

It is seen that, for all $\mu \in (0, H)$, we can choose a positive ρ such that the time derivative of W is negative definite in $E(\mu, \rho)$ and therefore is integrally unbounded. For example, using

$$\rho = \frac{-H + \sqrt{H^2 + \epsilon\mu^2/2}}{\epsilon} > 0 \quad (\text{A10})$$

in Eq. (A9) implies

$$\dot{W} \leq -\mu^2/2. \quad (\text{A11})$$

The above inequalities are sufficient conditions, guaranteeing that the fully synchronized state is globally asymptotically stable (see Theorem 5.7 and 5.8 in [37]). The assumption $1 \geq g_0|\sigma|$ together with $\sigma = \pm(1 - \kappa)$ implies Eq. (8).

-
- [1] H. Fujisaka and T. Yamada, *Prog. Theor. Phys.* **69**, 32 (1983).
- [2] V. S. Afraimovich, N. N. Verichev, and M. I. Rabinovich, *Radiophys. Quantum Electron.* **29**, 795 (1986).
- [3] L. M. Pecora and T. L. Carroll, *Phys. Rev. Lett.* **64**, 821 (1990).
- [4] A. Uchida, F. Rogister, J. García-Ojalvo, and R. Roy, *Progress in Optics* (North-Holland, Amsterdam, 2005), Vol. 48, pp. 203–342.
- [5] N. F. Rulkov, M. A. Vorontsov, and L. Illing, *Phys. Rev. Lett.* **89**, 277905 (2002).
- [6] T. Heil, I. Fischer, W. Elsässer, J. Mulet, and C. R. Mirasso, *Phys. Rev. Lett.* **86**, 795 (2001).
- [7] J. Mulet, C. Mirasso, T. Heil, and I. Fischer, *J. Opt. B: Quantum Semiclass. Opt.* **6**, 97 (2004).
- [8] M. C. Chiang, H. F. Chen, and J. M. Liu, *IEEE J. Quantum Electron.* **41**, 1333 (2005).
- [9] M. Y. Kim, R. Roy, J. L. Aron, T. W. Carr, and I. B. Schwartz, *Phys. Rev. Lett.* **94**, 088101 (2005).
- [10] I. B. Schwartz and L. B. Shaw, *Phys. Rev. E* **75**, 046207 (2007).
- [11] E. Klein, N. Gross, M. Rosenbluh, W. Kinzel, L. Khaykovich, and I. Kanter, *Phys. Rev. E* **73**, 066214 (2006).
- [12] R. Vicente, S. Tang, J. Mulet, C. R. Mirasso, and J.-M. Liu, *Phys. Rev. E* **73**, 047201 (2006).
- [13] I. Fischer, R. Vicente, J. M. Buldu, M. Peil, C. R. Mirasso, M. C. Torrent, and J. Garcia-Ojalvo, *Phys. Rev. Lett.* **97**, 123902 (2006).
- [14] J. K. White, M. Matus, and J. V. Moloney, *Phys. Rev. E* **65**, 036229 (2002).
- [15] L. Wu and S. Zhu, *Phys. Lett. A* **315**, 101 (2003).
- [16] E. A. Rogers-Dakin, J. Garcia-Ojalvo, D. J. DeShazer, and R. Roy, *Phys. Rev. E* **73**, 045201 (2006).
- [17] L. B. Shaw, I. B. Schwartz, E. A. Rogers, and R. Roy, *Chaos* **16**, 015111 (2006).
- [18] A. Englert, W. Kinzel, Y. Aviad, M. Butkovski, I. Reidler, M. Zigzag, I. Kanter, and M. Rosenbluh, *Phys. Rev. Lett.* **104**, 114102 (2010).
- [19] M. Peil, L. Larger, and I. Fischer, *Phys. Rev. E* **76**, 045201 (2007).
- [20] M. Peil, M. Jacquot, Y. K. Chembo, L. Larger, and T. Erneux, *Phys. Rev. E* **79**, 026208 (2009).
- [21] K. E. Callan, L. Illing, Z. Gao, D. J. Gauthier, and E. Schöll, *Phys. Rev. Lett.* **104**, 113901 (2010).
- [22] A. S. Landsman and I. B. Schwartz, *Phys. Rev. E* **75**, 026201 (2007).
- [23] J. Kestler, E. Kopelowitz, I. Kanter, and W. Kinzel, *Phys. Rev. E* **77**, 046209 (2008).
- [24] L. Illing and D. J. Gauthier, *Physica D* **210**, 180 (2005).
- [25] L. Illing and D. J. Gauthier, *Chaos* **16**, 033119 (2006).
- [26] T. E. Murphy, A. B. Cohen, B. Ravoori, K. R. B. Schmitt, A. V. Setty, F. Sorrentino, C. R. S. Williams, E. Ott, and R. Roy, *Philos. Trans. R. Soc. A* **368**, 343 (2010).
- [27] V. N. Belykh, G. V. Osipov, V. S. Petrov, J. A. K. Suykens, and J. Vandewalle, *Chaos* **18**, 037106 (2008).
- [28] N. F. Rulkov, M. M. Sushchik, L. S. Tsimring, and H. D. I. Abarbanel, *Phys. Rev. E* **51**, 980 (1995).
- [29] H. D. I. Abarbanel, N. F. Rulkov, and M. M. Sushchik, *Phys. Rev. E* **53**, 4528 (1996).
- [30] L. Illing, G. Hoth, L. Shareshian, and C. May, *Phys. Rev. E* **83**, 026107 (2011).
- [31] P. Ashwin, J. Buescu, and I. Stewart, *Nonlinearity* **9**, 703 (1996).
- [32] V. Flunkert, O. D’Huys, J. Danckaert, I. Fischer, and E. Schöll, *Phys. Rev. E* **79**, 065201 (2009).
- [33] H. D. I. Abarbanel and M. B. Kennel, *Phys. Rev. Lett.* **80**, 3153 (1998).
- [34] L. M. Pecora and T. L. Carroll, *Phys. Rev. Lett.* **80**, 2109 (1998).
- [35] T. Nishikawa and A. E. Motter, *Phys. Rev. E* **73**, 065106 (2006).
- [36] V. Flunkert, S. Yanchuk, T. Dahms, and E. Schöll, *Phys. Rev. Lett.* **105**, 254101 (2010).
- [37] V. B. Kolmanovskii and V. R. Nosov, *Stability of Functional Differential Equations*, Mathematics in Science and Engineering Vol. 180 (Academic Press, London, 1986).